Functional Materials 15, No.2 (2008)

Surface defects of BGO crystals

E.P.Galenin, I.V.Gerasymov, V.T.Nahornyak, O.Ts.Sidletskiy, S.A.Tkachenko

Institute for Scintillation Materials, STC "Institute for Single Crystals", National Academy of Sciences of Ukraine, 60 Lenin Ave., 60001 Kharkiv, Ukraine

Received January 18, 2008

The surface defects of $Bi_4Ge_3O_{12}$ crystals grown by Czochralski have been considered. The influence of the melt level lowering in the crucible and the growth atmosphere composition on the formation of defects have been described. A mechanism of defect formation has been proposed making in possible to judge of the crystallization front stability and morphology during the crystal growth and the presence of blocks in the crystals basing on the observed defect character.

Рассмотрены поверхностные дефекты кристаллов $Bi_4Ge_3O_{12}$, выращенных классическим методом Чохральского. Описано влияние уменьшения уровня расплава в тигле и состава среды выращивания на образование дефектов. Предложен механизм их возникновения, позволяющий по характеру дефектов судить о морфологии и стабильности фронта кристаллизации во время роста кристалла, размерах ячеек и наличии блоков в кристаллах.

Bismuth germanate $Bi_4Ge_3O_{12}$ (BGO) is an intrinsic undoped scintillator that exhibits a high efficiency of high-energy γ-quanta recording, a sufficient fast-action (300 ns) and is unhygroscopic. BGO is used successfully in the high energy physics (calorimeters, electromagnetic spectrometers), medicine (positron emission tomography, computer-aided tomography), in the radioactivity monitoring devices, geological survey, etc. [1].

The BGO crystals are grown from the melt in oxygen-containing atmospheres using mainly Czochralski techniques, both low-gradient [2] (the axial gradient at the crystallization front (CF) $G = 0.1$ to 1 K/cm) and classical [3] ($G \sim 50$ K/cm) ones. The oxygen-containing medium is used to prevent the melt de-stoichiometry [4]. The quality of BGO crystals is deteriorated due to the presence of defects therein, namely, inclusions of foreign phases that cause the crystal coloration and increased absorption of self-emission [5]; contamination of the crystals with platinum dissolved in the melt resulting in inhomogeneity of scintillation characteristics [6]; gas inclusions scattering the crystal self-emission [5–7].

In the mass production of BGO crystals, the crystal morphology is of a great importance, since it defined the material loss at processing and thus the production cost. Therefore, the production of crystals with the preset morphology is extremely important. F BGO crystals grown using Czochralski technique, the helical growth [7] and twisted form [4] are typical defects influencing the morphology. We have found that vertical recesses are formed at the BGO surface during the growing. The origins of those defects are not described in literature, therefore, are of interest to be studied. The purpose of this work is to study the origins and the formation mechanism of the vertical recesses at the crystal surface.

The BGO crystals were grown from platinum crucibles in the "Kristall 3M" apparatus with induction heating using the classical Czochralski technique. The crystals were of ∅57×200 mm^2 size, the pulling speed

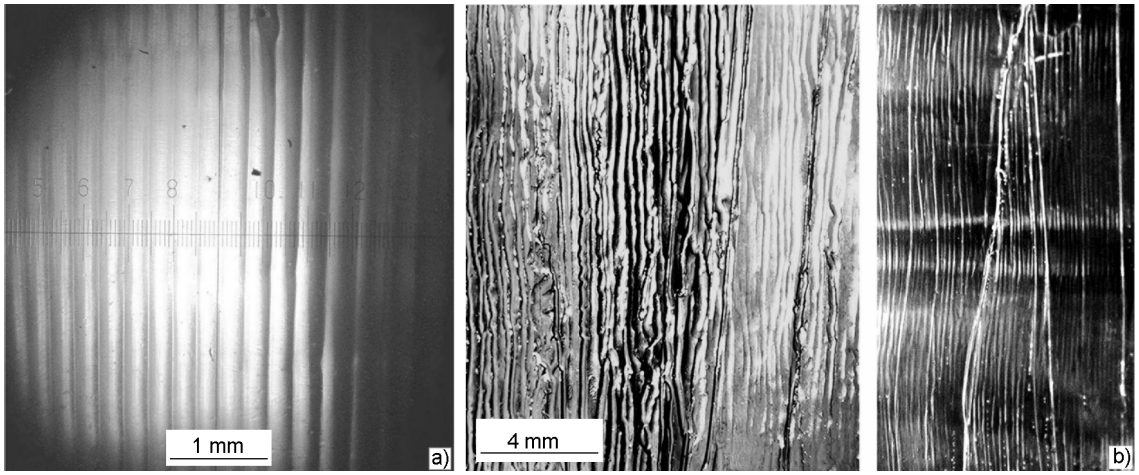

Fig. 1. Side surface defects of a BGO crystal: (a) straight lines at about 250 μm spacing (optical microscope); (b) sinuous and diverging lines.

was 1.2 mm/h, the rotation speed 35 to 45 rpm, the growing direction <100>; the axial gradient at the melt surface amounted about 50 K/cm. The growing was carried out in air or in argon/oxygen mixture with Ar content 85 % or more. The X-ray structure (XRD) and X-ray phase (XPA) examinations were carried out using a DRON 1 general purpose X-ray diffractometer (CuK_β, $\lambda = 1.39217$ Å). The crystal surface composition was studied by X-ray photoelectron spectroscopy (XPS) using a Kratos XPS-800 instrument (the residual pressure in the chamber $5 \cdot 10^{-9}$ Torr, MgK_α emission, $h\gamma = 1253.6$ eV). The optical transmission spectra were measured in the 190 to 1100 nm range using a double-beam SPECORD 40 spectrophotometer. The micro-impurity content was determined by the atomic emission spectroscopy using a DFS-8 diffraction spectrograph.

On the surface of the grown BGO crystals, we have observed linear vertical recesses (Fig. 1) of about 0.5 mm depth at the crystal top and up to 5 mm in its lower part. When the crystal was grown in air, the recesses were observed beginning at 45 to 90 mm from the cylindrical part; for crystals grown in argon/oxygen mixture, that distance was 5 to 50 mm. Thus, the appearance moment of the surface recesses depends considerably on the gas atmosphere where the crystal was grown. The recesses were continued up to the crystal end. In the upper crystal part, the 25 to 40 mm long recesses were shaped as parallel straight lines with a well-defined step of about 250 μm (Fig. 1a). Then, the recesses became sinuous and deeper, sometimes divergent or convergent (Fig. 1b). In the regions of

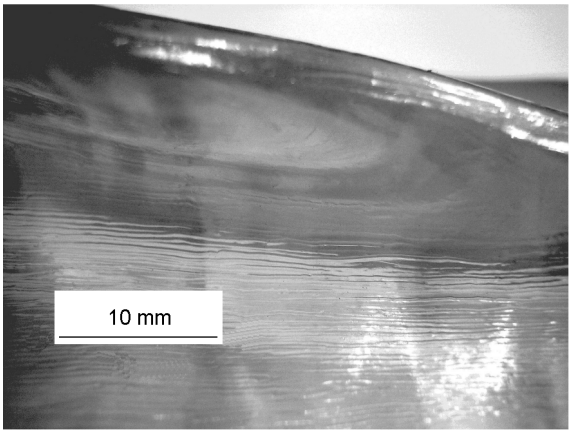

Fig. 2. Surface defects under a "wing".

crossed recesses, the XRD has revealed blocks with a 1° to 17° disorientation, the disorientation angle being coincident with the angle between the recess lines. The non-parallel recesses are appeared when the blocks in the crystal are formed and tapered. Thus, the recess direction is connected with the crystal structure perfection.

The surface defects were present also in the crystals of twisted morphology formed by wing-like spurs (Fig. 2). In such crystals, the vertical recesses on the spur inner surface are screened from the crucible wall radiation. Thus, the recesses cannot be supposed to appear due to the crystal surface melting resulting from overheating caused by the crucible wall radiation.

The oxygen content in the growth atmosphere influenced significantly the defect depth. The lower was the oxygen content in the gas medium, the deeper were the recesses (at O_2 concentration >1 %, up to 2 mm; at that <1 %, up to 5 mm). At a low oxygen content (0.5 % and less), inclusions

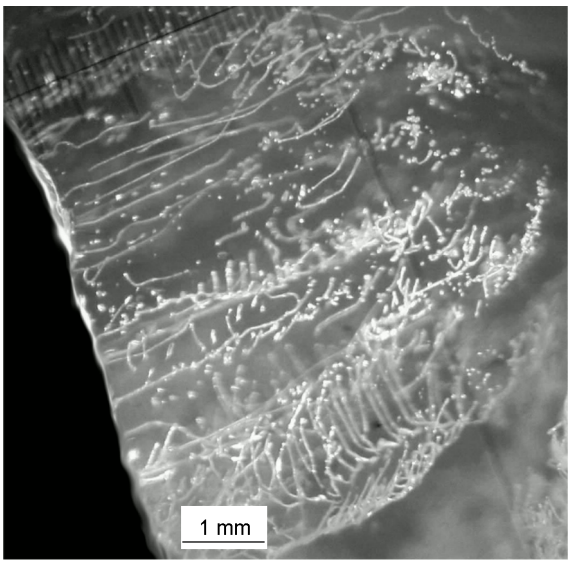

Fig. 3. Colored subsurface inclusions in a crystal.

arranged in rows were appeared at the surface of the crystal upper part (prior to the recesses formation). Lower, the vertical rows of near-surface inclusions were observed along with the recesses (Fig. 3). Those rows were outcropped to the surface within the vertical recesses. In crystals grown in atmospheres containing more than 1 % of oxygen, the inclusions at the surface were observed only seldom and the near-surface ones were absent at all.

The transmission spectrum of a sample containing the inclusions is presented in Fig. 4. The inclusions are seen to do not cause additional absorption centers but act as scattering centers.

To determine the inclusion composition using XPS, a comparative analysis of the cleavage surface of a defect-free crystal (Sample A) and of a surface containing the inclusions (Sample B) was conducted. The surface composition was determined from the area ratio under the lines of C1s, O1s, Bi4f, Ge3p core shells, taking into account the sensitivity factors. The analyzed layer was 5 nm thick. The atomic concentrations of elements at the sample surfaces are presented in Table 1 (the presence of carbon is due to adsorption of hydrocarbons at the sample surface).

The analytical data have shown that the surface containing the inclusions is enriched in bismuth oxide as compared to that of a defect-free crystal. Thus, the inclusions may consists of phases with stoichiometry deviated from the eulytine one towards the bismuth oxide. According to the phase diagram of Bi_2O_3–GeO_2 system [8], those

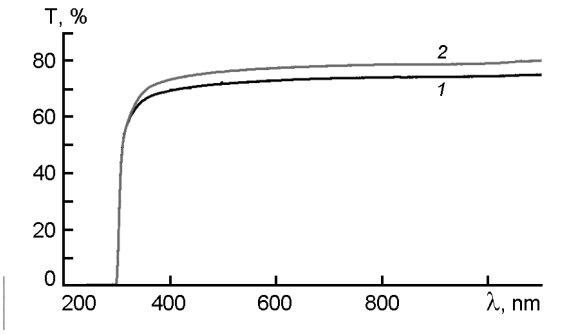

Fig. 4. Transmission spectra of BGO crystal; *1* – with inclusions, *2* – etalon.

Table 1. The atomic concentrations of elements at the sample surfaces.

Sample	C, at. %	O, at. %	Bi, at. %	Ge, at. %	Bi/Ge
A	66.1	24.0	6.5	3.4	1.9
B	71.8	15.8	9.8	2.6	3.8

Table 2. Typical micro-impurities in BGO melt.

Element	Content, wt. %	Element	Content, wt. %
Fe	$2\cdot10^{-4}$	Sn	$2\cdot10^{-4}$
Pb	$2\cdot10^{-4}$	Ni	$5\cdot10^{-5}$
Mg	$2\cdot10^{-4}$	Al	$2\cdot10^{-4}$
Si	$3\cdot10^{-4}$	Mo	$1\cdot10^{-5}$
Cr	$1\cdot10^{-5}$	Cu	$4\cdot10^{-4}$

phases can be sillenite $Bi_{12}GeO_{20}$ or a metastable Bi_2GeO_5 ones. The XPA has shown that the inclusions are formed by the polycrystalline metastable Bi_2GeO_5 phase. It can be formed in the diffusive melt layer at the CF of the crystal in growth [9]. Moreover, the Bi_2GeO_5 concentration can increase from the CF center towards its periphery due to centrifugal force and radial motion of the melt (caused by the crystal rotation). That is why the inclusions were formed on the surface of the crystal upper parts when those were grown at a great axial gradient. In the course of growth, the melt level is lowered and the CF is moved into the crucible depth, while the axial gradient decreases as the crystal is heated by the crucible wall radiation. In such conditions, the crystal surface temperature exceeds that of the metastable phase crystallization, thus, Bi_2GeO_5 inclusions are not crystallized at the surface. The low axial gradient, the

presence of micro-impurities (Table 2) and the metastable phase at the CF result in formation of cellular CF morphology [10].

As the cellular morphology of the CF is formed for the BGO crystals, the ribbed structure of the liquid/solid interface is a characteristic feature [11]. Therefore, the impurities are concentrated in recesses between the CF ribs at the growing crystal periphery, because the melt moves radially with respect to CF. The presence of Bi_2GeO_5 in the cell recesses hinders the growth of eulytine ($Bi_4Ge_3O_{12}$) crystal. Thus, the impurities block the crystal growth and provide the vertical recesses. As the axial gradient decreases and the metastable phase concentration in the melt increases during the growth, the surface defects become deeper. When the growth atmosphere is depleted of oxygen (0.5 %), the Bi_2GeO_5 concentration in the melt is increased so that the metastable phase is captured in the form of near-surface inclusions.

It follows from the above that the vertical recesses in the BGO crystal surface appear due to formation of cellular CF morphology in the presence of impurities. The impurities include both the micro-impurities in the initial components and the metastable Bi_2GeO_5 phase that is formed in the course of growth. It is just the metastable phase that plays the critical part in the formation of vertical recesses.

Thus, the formation of defects shaped as vertical recesses on the BGO crystal surface is caused by formation of the metastable Bi_2GeO_5 phase in the melt and the decreased axial gradient at the CF during the growth. The following mechanism of that phenomenon is proposed. At the BGO crystal growth, the formed metastable phase and decreased axial gradient at the CF cause the CF cellular morphology; the increased concentration of impurities in the recesses of cells at the CF periphery blocks the crystal growth, thus causing the vertical recesses on its surface. In the course of growth, the axial gradient decreases and the impurity concentration increases continuously, resulting in the increasing depth of the surface defects (from 0.5 up to 5 mm). The uniform spacing (250 μm) of the vertical recesses evidences the CF cell periodicity and the parallelism thereof confirms the constant CF morphology in the course of growth. As the blocks are formed or outcropped in the crystal, the CF cells become displaced, that is why the recesses become non-parallel. An increased concentration of metastable phase in the crystal (at oxygen content in the growth atmosphere less than 0.5 %) results in the Bi_2GeO_5 phase crystallization at the surface of the crystal upper part (when the axial gradient is high) and its capturing in the form of near-surface inclusions (when the gradient is low). The character of vertical recesses on the BGO crystal surface makes it possible also to judge of thermal conditions of the crystal growth, the crystal structure perfection and the CF cell size.

Authors are thankful to M.V.Dobrotvorskaya, V.F.Tkachenko, V.A.Tsurikov, Z.V.Shtitelman, V.V.Nesterkina who assisted in obtaining experimental data used in this work.

References

1. M.E.Globus, B.V.Grinyov, Inorganic Scintillators: Novel and Traditional Materials, Akta, Kharkov (2001).
2. Yu.A.Borovlev, N.V.Ivannikova, V.N.Shlegel et al., *J. Cryst. Growth*, **229**, 305 (2001).
3. S.F.Burachas, L.L.Nagornaya, G.M.Onyshchenko et al., *Semiconductor Physics, Quantum Electronics and Optoelectronics*, **3**, 237 (2000).
4. K.Takagi, T.Fukazawa, *J. Cryst. Growth*, **76**, 328 (1986).
5. F.Smet, W.J.P.Van Enckenvort, *J. Cryst. Growth*, **88**, 169 (1988).
6. F.Alegretti, R.Borgia, R.Riva, *J. Cryst. Growth*, **94**, 373 (1989).
7. A.Horovitz, G.Kramer, *J. Cryst. Growth*, **78**, 121 (1986).
8. F.Smet, W.J.P.Van Enckenvort, *J. Cryst. Growth*, **100**, 417 (1990).
9. V.P.Zhereb, V.M.Skorikov, *Neorg. Mater.*, **39**, 1365 (2003).
10. R.A.Laudise, The Growth of Single Crystals, Englewood Cliffs, New Jersy (1970).
11. E.P.Galenin, Ya.V.Gerasimov, S.A.Tkachenko, in: Abstr. Conf. on Crystal Physics of XXI Century, (2006), p.44.

Поверхневі дефекти кристалів BGO

Є.П.Галенін, Я.В.Герасимов, В.Т.Нагорняк, О.Ц.Сідлецький, С.А.Ткаченко

Розглянуто поверхневі дефекти кристалів $Bi_4Ge_3O_{12}$, вирощених методом Чохральського. Описано вплив зменшення рівню розплаву у тиглі й складу середовища вирощування на утворення дефектів. Запропоновано механізм їх виникнення, який дає можливість за характером дефектів оцінювати морфологію і стабільність фронту кристалізації під час росту кристала, наявність блоків у кристалах.